Current Research in Food Science 9 (2024) 100916

Contents lists available at ScienceDirect

Current Research in Food Science

journal homepage: www.sciencedirect.com/journal/current-research-in-food-science

Short Communication

Impact of covalent binding with p-coumaric acid on pea protein's structural and functional properties

Xuxiao Gong, Hyuk Choi, Yaqi Zhao, Qinchun Rao, Leqi Cui *

Department of Health, Nutrition, and Food Sciences, Florida State University, Tallahassee, FL, 32306, USA

ARTICLE INFO

Handling Editor: Dr. Quancai Sun

Keywords:
Pea protein
Phenolic acid
Conjugates
Solubility

ABSTRACT

This study investigated the effects of covalent bonding between pea protein isolate (PPI) and p-coumaric acid (p-CA) on the protein's secondary structure, solubility, foaming properties, emulsifying capacity, and thermal stability. Binding p-CA led to alterations in the secondary structure of PPI, including an increase in α-helix and random coil and a decrease in β-turn. Additionally, it resulted in a reduction in SH and NH groups, as well as a decrease in particle size. As the amount of bound p-CA increased, an increased tendency for aggregation was proposed, resulting in the formation of soluble aggregates through hydrophobic interactions, which was confirmed by a reduction in particle size of proteins after being dissolved in SDS. These structural modifications influenced the protein's functional properties, with the conjugates showing enhanced solubility and emulsifying capacity across various pH levels, but weaker foaming capacity and foam stability. Furthermore, the conjugates exhibited a lower initial denaturation temperature but a higher thermal denaturation enthalpy change (ΔH) compared to PPI, which may be attributed to protein unfolding and the formation of new covalent bonds. This study highlights the potential of p-CA covalent modification of PPI to enhance its functional properties, making it more suitable for food industry applications.

1. Introduction

Pea protein has garnered attention in the food industry due to its high yield, low cost, and nutritional value, increasingly serving as a substitute for soy protein (Schneider et al., 2023; Wang et al., 2022). However, pea protein application is hindered by its inferior functional properties, especially solubility, largely determined by its high content of globulins (Cui et al., 2020; Lu et al., 2020). Meanwhile, like other proteins, pea protein is susceptible to changes in environmental pH, which also limits its applications. To solve these issues, many studies are focused on chemically or physically modifying pea protein structure. For example, Zha et al. (Zha et al., 2019) reported that Maillard reaction between gum Arabic and pea protein can increase protein's solubility. High-intensity ultrasound has also been reported to enhance the solubility and foaming stability of pea protein (Gao et al., 2022). However, chemical modifications such as the Maillard reaction require strict control of the reaction process to prevent the formation of undesirable by-products (de Oliveira et al., 2016), and processing like ultrasound or high hydrostatic pressure face challenges in scaling up.

The interaction between polyphenols and proteins is increasingly applied to enhance food protein functionality. The polyphenol-protein interaction can be categorized under covalent (conjugate) and non-covalent (complex) bindings, where covalent bindings can be formed by oxidized phenolic acids or proteins to form more stable covalent bonds (Gong et al., 2023). Pi et al. (Pi et al., 2023) reported that the covalent bonding of soy protein with gallic acid, caffeic acid, and tannic acid improved the emulsifying activity of soy protein, based on changes in the protein secondary structure. The binding of walnut protein with ellagic acid or EGCG has also been reported to enhance protein solubility (Huang et al., 2022). Given those success in other proteins and that peas naturally contain phenolic compounds, modifying pea protein with phenolic acids is a reasonable approach.

In this study, we aim to investigate the potential of covalent bonds formed by phenolic acid and pea protein to improve the functionality of pea protein. Since p-coumaric acid (p-CA) is naturally present in plants and grains with simplified phenolic acid structure (Pei et al., 2016), which can minimize interference from additional side groups, this study opts to covalently bind p-CA to pea protein, exploring its potential in enhancing pea protein functionality. To achieve this, the impact of p-CA covalent binding on pea protein secondary structure and functional

* Corresponding author.
E-mail address: lcui2@fsu.edu (L. Cui).

https://doi.org/10.1016/j.crfs.2024.100916
Received 29 August 2024; Received in revised form 10 October 2024; Accepted 3 November 2024
Available online 5 November 2024

properties is investigated.

2. Materials and methods

2.1. Materials

Pea protein isolate (PPI) was purchased from Naked Nutrition (Miami, FL, USA). The protein content was 90 %, and the fat and carbohydrate content were 1 % and 7 %, respectively. P-Coumaric acid (p-CA), was purchased from Sigma (St. Louis, MO, USA). All other chemicals and reagents used in this study were of analytical grade and purchased from VWR (Chicago, IL, USA).

2.2. Preparation of PPI-p-CA conjugates

The preparation of the PPI-p-CA conjugates was carried out according to the method reported by Zhou et al. (Zhou et al., 2020) with slight modifications. PPI solution (PBS, pH 9.0) and p-CA solution (PBS, pH 9.0) were mixed and adjusted to pH 9.0 with 1 M NaOH. The mixture was stirred at 25 °C for 24 h before being dialyzed at 4 °C for 24 h to remove free p-CA. The dialyzed conjugates were freeze-dried to obtain the PPI-p-CA conjugate powder. Three initial polyphenol/protein ratios (0.5 mmol/g, 1 mmol/g, or 2 mmol/g) were prepared, which were named PCA1, PCA2, and PCA3, respectively, and PPI without p-CA addition was used as a control (Table 1).

2.3. Fourier transform infrared (FT-IR) spectroscopy

The infrared spectra were recorded using a FTIR-ATR (JASCO 6800, JASCO, Japan) with a 4 cm^{-1} resolution in the range of 4000–400 cm^{-1} (Cheng et al., 2024). The spectra were reported after noise elimination, baseline correction, and smoothing processing. Second derivatives and Gaussian curve fitting were obtained using Origin (OriginLab Corp., MA, US).

2.4. Determination of the binding groups

The amino and sulfhydryl groups were determined as the reactive groups for covalent binding (Gong et al., 2023). The amino groups were measured following Adler-Nissen (1979) 's method and using 0.02–0.4 mM leucine as the standard curve. The free sulfhydryl group was determined according to our previous method with no modifications (Cui et al., 2021).

2.5. Particle size, and polydispersity index

The particle size and polydispersity (PDI) of the samples were measured using a Zetasizer, following the procedure outlined in our previous work (Cheng et al., 2022) with no modifications.

2.6. Sodium dodecyl sulphate polyacrylamide gel electrophoresis (SDS-PAGE)

Non-reducing SDS-PAGE was performed to study the protein profiles according to Tang et al. (Tang et al., 2024). Each sample (0.5 mg protein/mL) was mixed (1:1 v/v) with 2 × non-reducing Laemmli sample buffer, followed by heating at 96 °C for 5 min. Each protein sample (3.75 μg/lane) was separated on a gel (4% stacking and 12% separating) using the running buffer (25 mM Tris, 192 mM glycine, and 0.1% (g/mL) SDS). The Precision Plus Protein Unstained Protein Standards (1610363, Bio-Rad Laboratories, Inc., Hercules, CA) were used for band sizing. After protein separation at 200 V for 1 h at 4 °C using a Mini-PROTEAN Tetra Electrophoresis Cell (Bio-Rad), the protein bands were visualized by Coomassie blue staining. The gel image was captured using Azure 600 Imaging System (Azure Biosystems, Inc., Dublin, CA) and analyzed using AzureSpot software (version 2.0.062, Azure Biosystems).

Table 1
Sample formulation and names.

Phenolic acid/protein ratio	Name
0.5 mmol/g	PCA1
1 mmol/g	PCA2
2 mmol/g	PCA3
0 mmol/g	PPI

2.7. Solubility

The percent protein solubility at pH 2–7 was determined according to our previous method (Cui et al., 2020), with slight modifications. First, the samples were dissolved in Citrate buffer (pH 2–7). The solutions (10 mg/mL) were vortexed at room temperature for 30 min and then stored at 4 °C overnight to ensure complete hydration. Afterward, the solutions were centrifuged at 11000*g for 10 min, and the protein concentration in the supernatant was measured by the BCA method. Samples were also dissolved in 0.1 M NaOH and processed using the same steps above to determine the total protein content. Protein solubility was calculated as the ratio of protein content in the supernatant to the total protein content.

2.8. Determination of total phenolic content

The total phenolic content of conjugates was measured using the Folin-Ciocalteu method (Ainsworth and Gillespie, 2007). A 100 μL sample was mixed with 200 μL 10 % Folin-Ciocalteu reagent. Then, 800 μL of 0.7 M Na_2CO_3 solution was added, and the mixture was incubated at room temperature in dark for 2 h. The absorbance of the mixture at 765 nm was measured by a BioTek Synergy H1 microplate reader, and the phenolic content was calculated by a standard curve prepared at 50–1000 nmol/mL of p-coumaric acid.

2.9. Foaming and emulsifying properties

The foaming capacity (FC) and stability (FS) were determined according to Cui et al. (Cui et al., 2020) with no modification. The emulsifying activity index (EAI) was determined following the method of Sadaf et al. (Sadaf et al., 2024). Briefly, oil-in-water emulsion was prepared using 0.1% PPI or conjugates, 1% corn oil, and 98.9% water. The mixture was homogenized at 13,000 rpm at room temperature for 3 min. Subsequently, 50 μL of the emulsion was added to 4.95 mL of 1% SDS solution. The absorbance (A) was measured at 500 nm, and the turbidity of the emulsion (T) was calculated using formula $T = (2.303\ A)/l$, where l is cuvette path length. The EAI was calculated using the following formula: $EAI = 2T/ØC$, where Ø is volume fraction of corn oil and C is protein concentration in the water phase (mg/mL).

2.10. Thermal stability

The thermal stability of PPI-p-CA conjugates was determined using differential scanning calorimetry (DSC). Briefly, 3 mg of samples were placed in crucibles with lids. The thermal analysis was conducted from 20 °C to 200 °C at a constant rate of 10 °C/min under an argon atmosphere with a flow rate of 100 mL/min. An empty crucible was used as a reference.

2.11. Statistical analysis

All measurements were performed on triplicate samples. The means were analyzed by analysis of variance (ANOVA) using SPSS, and the differences between mean values were compared using the Duncan test with a significant level of $P < 0.05$.

3. Results and discussion

3.1. FT-IR spectra

Protein structural changes after binding p-CA were determined using FTIR. Fig. 1A showed that the addition of p-CA affects the protein spectra primarily in the amide I region (1600–1700 cm^{-1}) and amide II region (1500–1600 cm^{-1}), which is related to the secondary structure of proteins. Also, the peak at 3000-3300 cm^{-1} is attributed to -OH stretching vibration (Movasaghi et al., 2008). The higher intensity of conjugates in this region compared to PPI suggests that the hydrogen bonding in the protein was enhanced through binding with p-CA. Next, we performed second-derivative analysis on the FTIR spectra (Fig. 1B–E) and assigned the secondary structure peaks according to previous work (Cheng and Cui, 2021), as shown in Table 2. Table 2 showed that addition of p-CA led to an increase in α-helix and random coil and a decrease in β-turn, while β-sheet and anti-parallel β-sheet remained almost unaffected. Overall, the above structural changes are expected to alter protein functional properties. For example, because α-helix, β-sheet, and random coil are maintained by hydrogen bonds, the differences in these structures between the conjugates and PPI indicated altered interactions with water molecules, which could affect protein

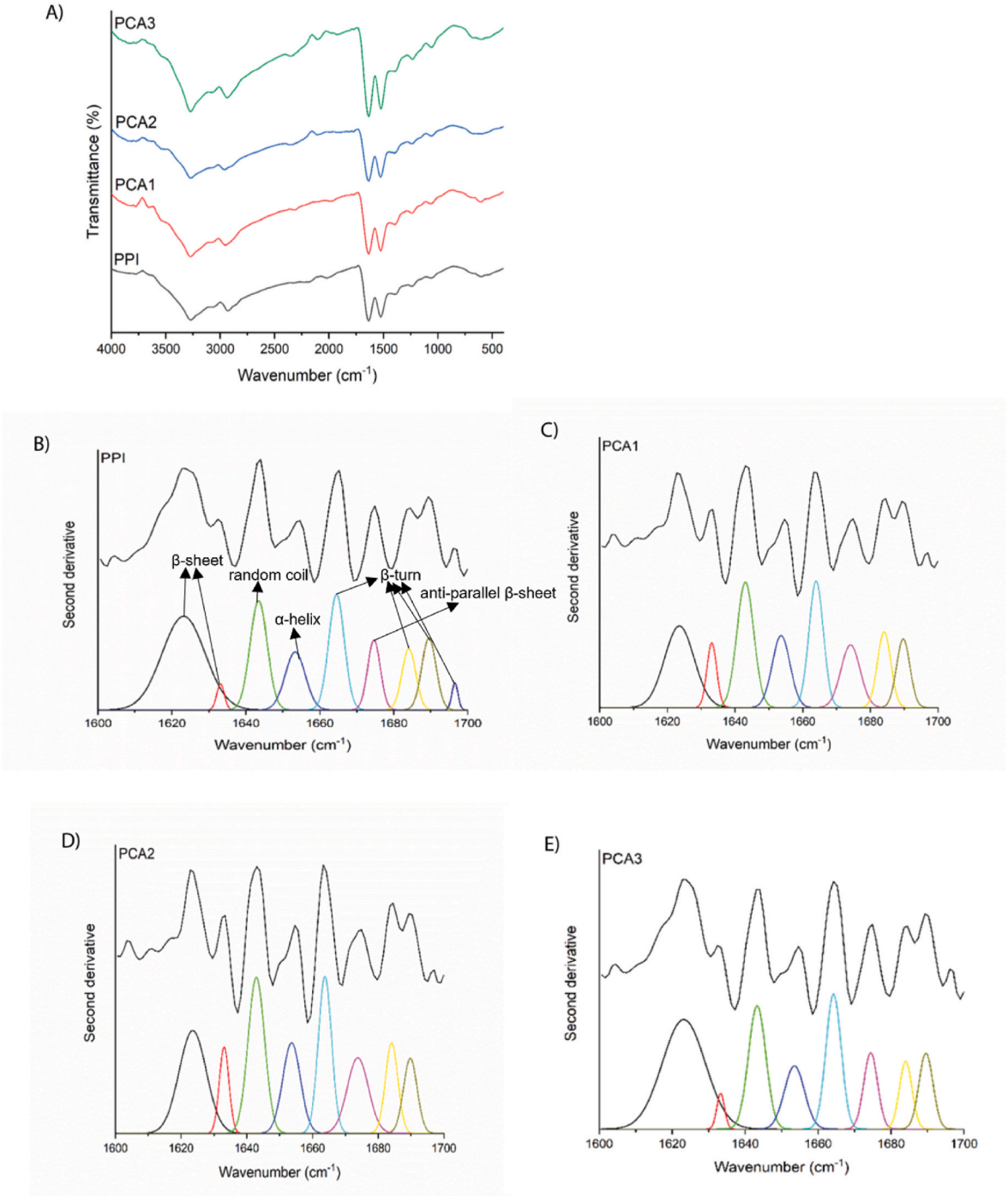

Fig. 1. The FTIR spectra (A), and second derivatives of amide I region (1600–1700 cm^{-1}) (B–E) of PPI and conjugates. For sample name abbreviations refer to Table 1.

Table 2
The secondary structure of PPI and conjugates.

	α-helix (%)	β-sheet (%)	Anti-parallel β-sheet (%)	β-turn (%)	Random coil (%)
PPI	6.33 ± 0.5[a]	39.35 ± 5.90[b]	14.58 ± 0.17[a]	25.01 ± 0.06[b]	14.92 ± 1.05[a]
PCA1	11.29 ± 0.35[c]	30.91 ± 0.17[ab]	14.00 ± 0.18[a]	24.38 ± 0.37[b]	19.24 ± 0.12[b]
PCA2	11.74 ± 0.07[c]	26.86 ± 0.45[a]	19.84 ± 0.21[b]	22.56 ± 0.20[a]	19.00 ± 0.02[b]
PCA3	9.41 ± 0.27[b]	37.02 ± 0.17[ab]	14.41 ± 0.25[a]	23.16 ± 0.05[a]	15.73 ± 0.24[a]

*Different letters indicate significant difference within the same column ($P < 0.05$).

solubility (Pace et al., 2014).

3.2. Reactive groups, particle size and SDS-PAGE

p-CA can covalently bind sulfhydryl (-SH) and amino (-NH) groups. As shown in Fig. 2A, with the increasing p-CA, the concentration of -SH and -NH in the conjugates decreased, indicating that the -SH and -NH groups in PPI participate in the formation of the conjugates. Moreover, the relative changes between PPI and PCA1 in -SH content (75 %) and -NH content (64 %) suggest that conjugation primarily occurs with -SH. Xu et al. (Xu et al., 2024) reported that the reaction of -SH with tannic acid occurs earlier than with -NH, supporting the notion that -SH has higher reactivity during the binding of proteins with phenolic acids.

Dynamic light scattering (DLS) measurements failed to provide particle size information due to the presence of large particles even after we filtered the sample solution. Our preliminary data (not shown) confirmed the unfolding of PPI-p-CA conjugates, and we suspected that the exposure of hydrophobic regions due to unfolding led to strong hydrophobic interactions among protein molecules, causing aggregation. Considering that SDS can dissociate protein aggregates by binding to hydrophobic regions and imparting negative charges, without affecting covalent bonds, we proposed to use DLS to measure the particle size of SDS-dissolved samples. Fig. 2 showed the particle size and PDI (Fig. 2B), and SDS-PAGE profile (Fig. 2C) of the SDS-dissolved conjugates and PPI. No significant difference in particle size between PCA1 and PPI was found, while the particle size decreased progressively from PCA2 to PCA3. With decreased particle size of SDS-dissolved conjugates, we expected more fractions of lower molecular weight subunits in the conjugates. However, the SDS-PAGE profiles of the conjugates remain unchanged compared to PPI (Fig. 2C). This observation that proteins, after SDS dissociation, had identical SDS-PAGE profiles but different particle sizes means that the subunits of PPI and conjugates with the same molecular weight (as shown in SDS-PAGE) could still show different tendencies of aggregation (as indicated by different particle sizes). We propose this was due to their different amount of available hydrophobic regions. It has been reported that in SDS solution, the hydrophobic region of unfolded proteins can interact with SDS to form a necklace-and-beads configuration, where the overall shape of the protein changes depending on the number and location of SDS micelles (Winogradoff et al., 2020). For proteins of the same molecular weight, those wrapped by more SDS molecules would have a smaller hydrated radius, resulting in a lower particle size measurement (Winogradoff et al., 2020). Because SDS binds to hydrophobic regions of proteins, the smaller particle size of conjugates in SDS solution could be due to greater exposure of hydrophobic regions, which further suggests that the driving force behind the aggregation of our original samples in the absence of SDS is also hydrophobic interaction.

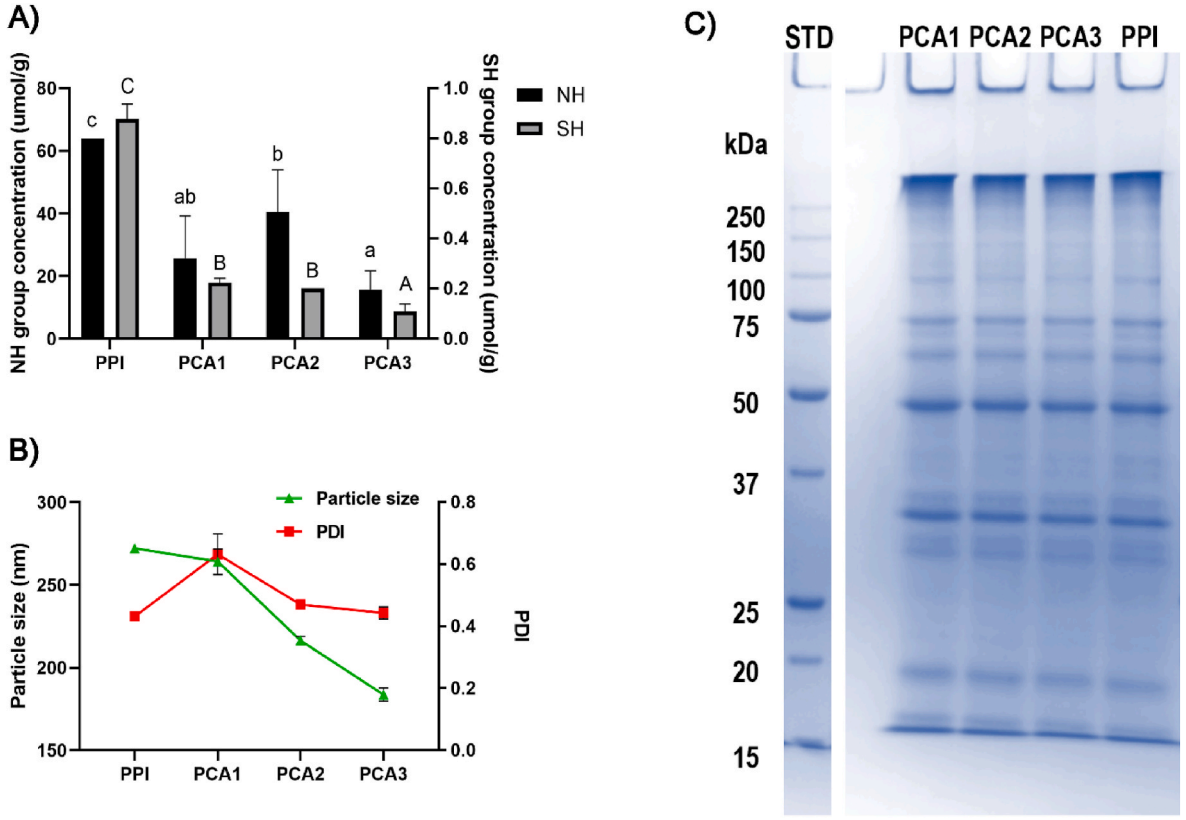

Fig. 2. The reactive groups (-NH left y axis, and -SH right y axis, A), particle size (left y axis, B), polydispersity index (PDI, right y axis, B), and SDS-PAGE protein profile (C) of PPI and conjugates. Different letters indicate significant difference ($P < 0.05$). For sample name abbreviations refer to Table 1.

3.3. Solubility and bonded p-CA content

Fig. 3A showed the solubility of PPI-p-CA conjugates under different pH conditions. Addition of p-CA increased the solubility of PCA2 and PCA3 at all tested pHs. It can be inferred that the unfolding of the protein structure increases the surface area of the conjugates to be in contact with water molecules, enhancing the opportunity for hydration layer formation among protein molecules (Srinivasan and KrikParkin, 2017). However, the unfolding of protein structure will also expose internal hydrophobic groups, which explains why PCA1 exhibited lower solubility than PPI at pH 2, 3, 6, and 7. Our preliminary result (data not shown) found that PCA1 had the highest surface hydrophobicity, thus the amount of p-CA bound to PCA1 could be insufficient to improve its overall solubility. Additionally, binding p-CA introduces hydrophilic hydroxyl and carboxyl groups, which may affect the solubility of conjugates due to hydrogen bonding between these groups and water molecules. Another interesting finding from Fig. 3A was that for the same conjugates, especially PCA2 and PCA3, their solubility was less affected by changing environmental pHs as compared to PPI. One explanation is that conjugates PCA2 and PCA3 are already unfolded and the bonded p-CA hinders further unfolding or refolding of conjugates when exposed to different environmental pHs. So, under different environmental pHs, PCA2 and PCA3 undergo little structural change, which could result in minimal influence on protein solubility.

The bonded amount of p-CA in conjugates at various pHs is shown in Fig. 3B. It would be reasonable to assume that when the same sample is exposed to different environmental pHs, there would be different amount of detectable p-CA concentrations because of their different solubility at pH 2–7. However, as shown in Fig. 3B, the change in p-CA concentration for the same sample at various pHs was smaller than the corresponding change in solubility. For example, for PCA2, its solubility went from ~15% at pH 4–~30% at pH 7 (a 100% increase); whereas its detectable p-CA content went from 0.113 mmol/g to 0.141 mmol/g (a 25% increase). Similarly, the p-CA concentration in PCA3 increased 10% from 0.238 mmol/g at pH 4 to 0.261 mmol/g at pH 7 whilst its solubility increased 50%. This observation suggested that the p-CA-bonded fraction of protein was already highly solubilized at various pHs, and the observed change of protein solubility in Fig. 3A at various pHs was caused by the unbonded fraction of protein.

3.4. Foaming properties, emulsifying capacity, and thermal stability

Fig. 3C showed that the addition of p-CA led to a decrease in protein foaming capacity and stability. This indicated that p-CA altered the distribution of protein's hydrophobic and hydrophilic regions by unfolding protein structure and introducing hydrophilic groups in such a way that worsened conjugates position at air-water interface (Fei et al., 2022). Also, the aggregation of conjugates could further disrupt the balance of the conjugates at the air-water interface, resulting in poor foaming stability. However, PCA3 showed higher foaming capacity than PCA1 and 2, suggesting that higher amounts of p-CA mitigated the decreased foaming capacity.

The emulsifying ability of all samples were measured as EAI (Fig. 3D). The conjugates exhibited inconsistent patterns of emulsifying capacity compared to PPI across different pH levels. For example, at pH 5 all conjugates showed weaker emulsifying capacity than PPI, but at pH 2, 3, 4, and 7, there was at least one conjugate that demonstrated better emulsifying capacity than PPI. No trend was observed among the conjugates with increasing p-CA either. For example, at pH 5 there was no significant difference among the conjugates, but at pH 3 emulsifying capacity decreased with increasing p-CA. The negative impact of excess phenolic acids on protein emulsifying ability has been reported (Kim et al., 2024). We suspected this negative impact was related to protein's ability to alter the environment pH. To test this, we measured the actual pH of the emulsion as shown in Fig. 3E. Note that emulsions were prepared using water phase at pH 2–7 initially (left y axis, dark grey), but PPI and conjugates all showed buffering effect as evidenced by the actual pH of the emulsion (right y axis, light grey). For example, for PPI stabilized emulsion, the initial pH was 3 but actual final pH is around 6.8. By contrast, for PPI-p-CA conjugate stabilized emulsions, the actual final pHs were around 3.5. This difference in the actual pH of the emulsion well explained why conjugates showed different EAI as compared to PPI.

Fig. 4 showed the differential scanning calorimetry (DSC)

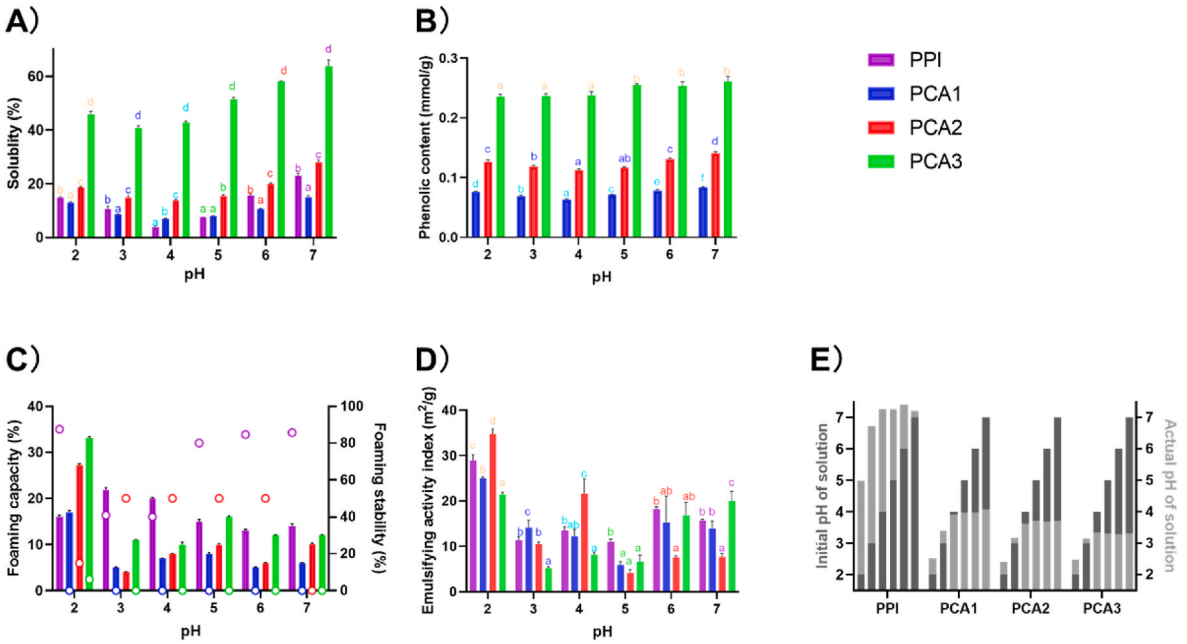

Fig. 3. The impact of binding p-coumaric acid on the functional properties of PPI and conjugates. A) Solubility. B) Phenolic content. C) Foaming capacity (bar, left y axis), and foaming stability (hollow circle, right y axis). D) Emulsifying activity index (EAI). E) The initial pH of solution (left y axis), and the actual pH of solution (right y axis). For B), different letters indicate significant difference among the same conjugate ($P < 0.05$). For the others, different letters indicate significant difference among the same pH ($P < 0.05$). For sample name abbreviations refer to Table 1.

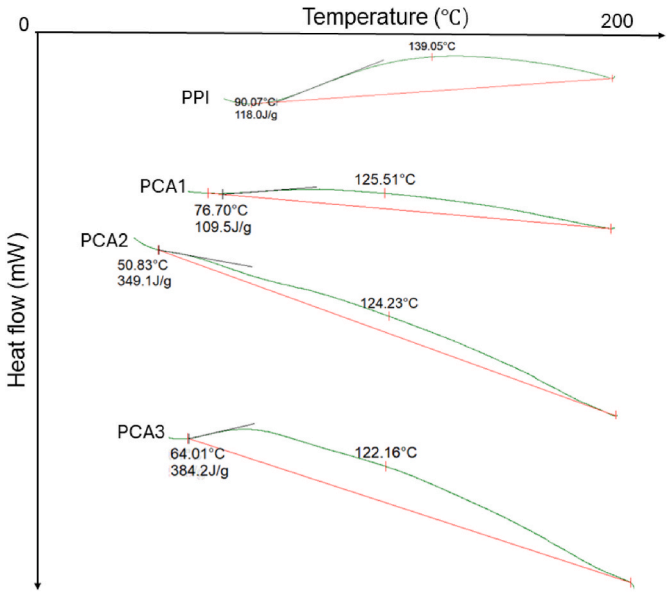

Fig. 4. The differential scanning calorimetry thermograms of PPI and conjugates, initial denaturation temperature, melting temperature, and ΔH were marked in the diagram. For sample name abbreviations refer to Table 1.

thermograms, including the initial denaturation temperature, melting temperature, and ΔH. The thermograms of all samples displayed a single endothermic peak. The initial denaturation temperature of all conjugates was lower than PPI, which could be due to that conjugates were more unfolded compared to PPI, making them more susceptible to heat. Additionally, the ΔH of the PCA2 and PCA3 were higher than PPI, which suggested the covalent bonds between p-CA and PPI required more energy to fully denature the conjugates.

4. Conclusions

In this study, p-CA modified PPI structure through covalent bonding, producing conjugates with enhanced solubility, while a high ΔH reflects increased thermal resistance. Depending on the amount of bonded P-CA and environmental pH, the foaming and emulsifying capacity were influenced differently. This study demonstrates the feasibility of using phenolic acids to improve the functionalities of pea protein isolates.

CRediT authorship contribution statement

Xuxiao Gong: Investigation, Formal analysis, Writing – original draft, preparation. **Hyuk Choi:** Investigation, Formal analysis. **Yaqi Zhao:** Investigation, Formal analysis. **Qinchun Rao:** Conceptualization, Formal analysis. **Leqi Cui:** Conceptualization, Supervision, Writing – review & editing.

Funding

This work was supported by the Pulse Crop Health Initiative program of the United States Department of Agriculture (USDA-ARS, No. 445000).

Declaration of competing interest

There are no conflicts to declare.

Data availability

Data will be made available on request.

References

Adler-Nissen, J., 1979. Determination of the degree of hydrolysis of food protein hydrolysates by trinitrobenzenesulfonic acid. J. Agric. Food Chem. 27 (6), 1256–1262.
Ainsworth, E.A., Gillespie, K.M., 2007. Estimation of total phenolic content and other oxidation substrates in plant tissues using Folin-Ciocalteu reagent. Nat. Protoc. 2 (4), 875–877.
Cheng, J., Cui, L., 2021. Effects of high-intensity ultrasound on the structural, optical, mechanical and physicochemical properties of pea protein isolate-based edible film. Ultrason. Sonochem. 80, 105809.
Cheng, J., Li, Z., Wang, J., Zhu, Z., Yi, J., Chen, B., Cui, L., 2022. Structural characteristics of pea protein isolate (PPI) modified by high-pressure homogenization and its relation to the packaging properties of PPI edible film. Food Chem. 388, 132974.
Cheng, J., Velez, F.J., Singh, P., Cui, L., 2024. Fabrication, characterization, and application of pea protein-based edible film enhanced by oregano essential oil (OEO) micro- or nano-emulsion. Curr. Res. Food Sci. 8, 100705.
Cui, L., Bandillo, N., Wang, Y., Ohm, J.-B., Chen, B., Rao, J., 2020. Functionality and structure of yellow pea protein isolate as affected by cultivars and extraction pH. Food Hydrocolloids 108, 106008.
Cui, L., Kimmel, J., Zhou, L., Chen, B., Rao, J., 2021. Improving the functionality of pea protein isolate through co-spray drying with emulsifying salt or disaccharide. Food Hydrocolloids 113, 106534.
de Oliveira, F.C., Coimbra, J.S.d.R., de Oliveira, E.B., Zuñiga, A.D.G., Rojas, E.E.G., 2016. Food protein-polysaccharide conjugates obtained via the maillard reaction: a review. Crit. Rev. Food Sci. Nutr. 56 (7), 1108–1125.
Fei, P., Zhang, Z., Wu, Y., Xiao, L., Zhuang, Y., Ding, N., Huang, B., 2022. Non-radical synthesis of amide chitosan with p-coumaric acid and caffeic acid and its application in pork preservation. Int. J. Biol. Macromol. 222, 1778–1788.
Gao, K., Zha, F., Yang, Z., Rao, J., Chen, B., 2022. Structure characteristics and functionality of water-soluble fraction from high-intensity ultrasound treated pea protein isolate. Food Hydrocolloids 125, 107409.
Gong, X., Sun, Q., Wang, X., Zhang, R., Peng, Y., Cui, L., 2023. Recent advances in pulse protein conjugation and complexation with polyphenols: an emerging approach to improve protein functionality and health benefits. Crit. Rev. Food Sci. Nutr. 1–11.
Huang, X., Yan, C., Lin, M., He, C., Xu, Y., Huang, Y., Zhou, Z., 2022. The effects of conjugation of walnut protein isolate with polyphenols on protein solubility, antioxidant activity, and emulsifying properties. Food Res. Int. 161, 111910.
Kim, W., Wang, Y., Selomulya, C., 2024. Emerging technologies to improve plant protein functionality with protein-polyphenol interactions. Trends Food Sci. Technol. 147, 104469.
Lu, Z.X., He, J.F., Zhang, Y.C., Bing, D.J., 2020. Composition, physicochemical properties of pea protein and its application in functional foods. Crit. Rev. Food Sci. Nutr. 60 (15), 2593–2605.
Movasaghi, Z., Rehman, S., ur Rehman, D.I., 2008. Fourier transform infrared (FTIR) spectroscopy of biological tissues. Appl. Spectrosc. Rev. 43 (2), 134–179.
Pace, C.N., Fu, H., Lee Fryar, K., Landua, J., Trevino, S.R., Schell, D., Grimsley, G.R., 2014. Contribution of hydrogen bonds to protein stability, 23 (5), 652–661.
Pei, K., Ou, J., Huang, J., Ou, S., 2016. p-Coumaric acid and its conjugates: dietary sources, pharmacokinetic properties and biological activities. J. Sci. Food Agric. 96 (9), 2952–2962.
Pi, X., Liu, J., Sun, Y., Ban, Q., Cheng, J., Guo, M., 2023. Protein modification, IgE binding capacity, and functional properties of soybean protein upon conjugation with polyphenols. Food Chem. 405, 134820.
Sadaf, N., Tuhanioglu, A., Hettiarachchy, N., Ubeyitogullari, A., 2024. Effect of a novel drying method based on supercritical carbon dioxide on the physicochemical properties of sorghum proteins. RSC Adv. 14 (9), 5851–5862.
Schneider, A.A., Bu, F., Ismail, B.P., 2023. Enhancement of pea protein solubility and thermal stability for acidic beverage applications via endogenous Maillard-induced glycation and chromatography purification. Curr. Res. Food Sci. 6, 100452.
Srinivasan, D., Krik, L., Parkin, 2017. Fennema's Food Chemistry.
Tang, C., Jiang, X., Liu, C., Washburn, B.K., Sathe, S.K., Rao, Q., 2024. Effect of temperature on structural configuration and immunoreactivity of pH-stressed soybean (*Glycine max*) agglutinin. Food Chem. 442, 138376.
Wang, J., Kadyan, S., Ukhanov, V., Cheng, J., Nagpal, R., Cui, L., 2022. Recent advances in the health benefits of pea protein (Pisum sativum): bioactive peptides and the interaction with the gut microbiome. Curr. Opin. Food Sci. 48, 100944.
Winogradoff, D., John, S., Aksimentiev, A., 2020. Protein unfolding by SDS: the microscopic mechanisms and the properties of the SDS-protein assembly. Nanoscale 12 (9), 5422–5434.
Xu, Q.-D., Yu, Z.-L., He, Q., Zeng, W.-C., 2024. Creating and characteristics of a novel biomacromolecules complex of pea protein isolated-tannic acid-magnesium ion. Int. J. Biol. Macromol. 276, 133939.
Zha, F., Dong, S., Rao, J., Chen, B., 2019. The structural modification of pea protein concentrate with gum Arabic by controlled Maillard reaction enhances its functional properties and flavor attributes. Food Hydrocolloids 92, 30–40.
Zhou, S.-D., Lin, Y.-F., Xu, X., Meng, L., Dong, M.-S., 2020. Effect of non-covalent and covalent complexation of (−)-epigallocatechin gallate with soybean protein isolate on protein structure and in vitro digestion characteristics. Food Chem. 309, 125718.